Water ingress in Y-type zeolite: Anomalous moisture-dependent transport diffusivity

Eduardo N. de Azevedo,[1] D. Vitoreti da Silva,[2] R. E. de Souza,[2] and M. Engelsberg[2]
[1]*Programa de Pós-Graduação em Ciência de Materiais, Universidade Federal de Pernambuco, Cidade Universitária, 50.670-901, Recife, Pernambuco, Brazil and*
[2]*Departamento de Física, Universidade Federal de Pernambuco, Cidade Universitária, 50.670-901, Recife, Pernambuco, Brazil*
(Received 12 April 2006; published 9 October 2006)

Nuclear magnetic resonance imaging measurements of liquid water ingress in a large number of nonactivated Y-type (Na) zeolite samples prepared under different conditions are reported on. Using an experimental arrangement that permits the application of Boltzmann's transformation of the 1D (one-dimensional) diffusion equation, the spatiotemporal scaling variables required for a collapse of the measured profiles into universal curves revealed subdiffusive behavior in all cases. It is shown that the one-dimensional fractal time diffusion equation constitutes a powerful tool to analyze the data and provides a connection between the moisture dependence of the effective transport diffusivities and the shapes of the universal curves. Thus, even for anomalous diffusion, the relationship between the universal curves and structural characteristics of the system; such as porosity, tortuosity of the pore space and, in some cases, the interplay between mesopores and nanopores can be addressed.

DOI: 10.1103/PhysRevE.74.041108 PACS number(s): 05.60.Cd, 05.40.−a, 82.56.Lz

I. INTRODUCTION

Water ingress in porous systems has been found, in many cases, to obey a diffusion equation with a concentration-dependent transport diffusivity. From an experimental point of view nuclear magnetic resonance (NMR) imaging has been particularly useful to monitor water ingress in porous systems under nonequilibrium conditions created by a concentration gradient. Since it is often feasible to approximate the conditions for the applicability of Boltzmann's transformation of the 1D (one-dimensional) diffusion equation [1] it is possible to verify whether moisture profiles actually scale as $x/t^{\gamma/2}$ with $\gamma=1$, as expected for normal diffusion. If the profiles indeed collapse into a single universal curve when plotted as a function of $x/t^{0.5}$, it is further possible to determine, from the universal curve, a moisture-dependent transport diffusivity [1,2].

We have recently demonstrated [3] that the procedure can be generalized to include also anomalous diffusion of a subdiffusive type. If one adopts a fractal time diffusion (FTD) equation [4–10] with boundary conditions suitable for Boltzmann's transformation it is possible to determine, even for anomalous diffusion, the moisture dependence of the generalized transport diffusivity from a universal curve where the scaling variable is $x/t^{\gamma/2}(\gamma<1)$.

Zeolites are classified as *X* or *Y* depending upon the ratio $n_{\mathrm{Si}}/n_{\mathrm{Al}}$ of silicon to aluminum in their faujasite crystal structure [11]. According to Beck [12] zeolites are considered to be of *X* type for ratios $n_{\mathrm{Si}}/n_{\mathrm{Al}}\leqslant 1.5$ whereas high silica zeolites with ratios $n_{\mathrm{Si}}/n_{\mathrm{Al}}>1.5$ are considered to be of *Y* type. Although *X* and *Y* zeolites share the same crystal framework they differ in some aspects. Typical crystal sizes in *X* zeolites, for example, are larger than in *Y* zeolites and there is also a characteristic difference in their hydrothermal behavior [11].

The sodalite cages in the faujasite structure form relatively large nanopores permitting molecules to diffuse in and out. These cages can only be formed in the presence of aluminate ions requiring that a charge-compensating cation, such as Na, also enters the chemical composition of the aluminosilicate.

Given the many applications of zeolites, diffusion in these systems has attracted considerable attention in recent years [13]. In spite of this effort some aspects of the problem are still not entirely solved. Especially those concerning the relationship between the diffusivity measured under a concentration gradient by NMR imaging, namely the transport diffusivity, and the self-diffusion coefficient measured under equilibrium conditions for example by the NMR pulse field-gradient (PFG) method [14–16]. Although, at a molecular level, transport diffusivity and self-diffusion originate in the same stochastic process and should be related to each other, the former contains an additional factor reflecting the concentration dependence of the chemical potential of the diffusers [17]. This is often the dominant effect in water transport in a porous system and manifests itself, on a macroscopic scale, through surface tension and capillary suction.

For a Y-type (Na) nonactivated zeolite we have recently [3] measured, using NMR imaging, moisture profiles resulting from water ingress from an external liquid water reservoir, approximating the conditions for the validity of Boltzmann's transformation. Scaling variables $x/t^{\gamma/2}$ with $\gamma<1$, suggesting subdiffusive behavior, were found for most systems studied. In some cases values of γ as small as 0.36 ± 0.04 were observed for the initial regime of water ingress. Moreover, not only the value of γ for a particular system, but also the moisture dependence of the effective transport diffusivity was found to be dependent upon the history and thermal treatment of the zeolite sample. Although different from the effects presented here, it is worth noticing that subdiffusive transport of some molecules through zeolite nanopores has also been reported in connection with self-diffusion measurements using the PFG method [18]. This behavior has been attributed to single-file diffusion [18–20].

In this work we extend the scope of our analysis of water ingress in nonactivated zeolites by considering a much wider

time domain, a variety of thermal treatments, and differently prepared Y-type (Na) zeolite samples. From the values of γ obtained we conclude that the behavior is always subdiffusive and that the transport diffusivities exhibit a rich variety of moisture dependences which in, some cases, reflect the interplay between intracrystallite nanopore adsorption and intercrystallite mesopore transport.

II. NORMAL DIFFUSION: MOISTURE DEPENDENCE OF THE TRANSPORT DIFFUSIVITY

Given the complexity of transport in porous systems under the action of concentration gradients a macroscopic hydrodynamic approach based on Darcy's law [21] is often adopted rather than a molecular description. Compared with simple porous systems zeolites are in a special category because in addition to liquid and vapor transport in the intercrystallite mesopores one has also to consider the adsorption of water molecules within intracrystallite nanopores.

Consider first a simple porous system, consisting of a solid matrix and a network of interparticle pores of micrometric size containing islands of liquid water as well as a vapor/air phase. One can define macroscopic average quantities within a representative elementary volume [22] (REV), typically several microns in size, which as a result of a variety of constrictions, contains a distribution of different pore diameters. An important macroscopic quantity is p_c, the average difference of capillary pressure between liquid, water, and air/vapor in a REV. Given that the pore diameter of a liquid island determines the difference in capillary pressure at the liquid-air/vapor interface, p_c will be a function of liquid water concentration W. The latter is defined as the volume of liquid within the REV divided by the volume of the REV whereas W_0 denotes the concentration of liquid water corresponding to saturation of all pores.

Since the wetting fluid in an unsaturated porous system fills in first the narrower pores, a significant tortuosity of the pore space, characterized by a broad distribution of pore diameters, leads to a large monotonic nonlinear increase of p_c with W [23]. For an unsaturated porous system with wetting walls $p_c(W)$ is negative and is expected to increase toward zero as the saturation concentration W_0 is reached. Furthermore, given that the gradient of average capillary pressure difference $-\partial p_c/\partial x = -(\partial p_c/\partial W)(\partial W/\partial x)$ is the driving force in Darcy's law, and assuming mass conservation and equal rates of liquid evaporation and vapor condensation, $W(x,t)$ can be shown [22,24,25] to obey a normal nonlinear diffusion equation for moisture transport. For 1D it takes the form:

$$\frac{\partial W(x,t)}{\partial t} = \frac{\partial}{\partial x}\left(D(W)\frac{\partial W(x,t)}{\partial x}\right), \tag{1}$$

where, from Darcy's law, the moisture-dependent transport diffusivity $D(W)$ should be proportional to the to the quantity $\partial p_c/\partial W$.

By approaching the boundary conditions suitable for Boltzmann's transformation of the diffusion equation it is possible to obtain, from measured moisture profiles $W(x,t)$, the moisture dependence $D(W)$ of the transport diffusivity [1]. Moreover, $D(W)$ is expected to be determined by the distribution function of pore diameters [23], with a steeper variation corresponding to a broader distribution. However, the theoretical basis needed for quantitative predictions based upon the structure of the porous system still needs to be improved.

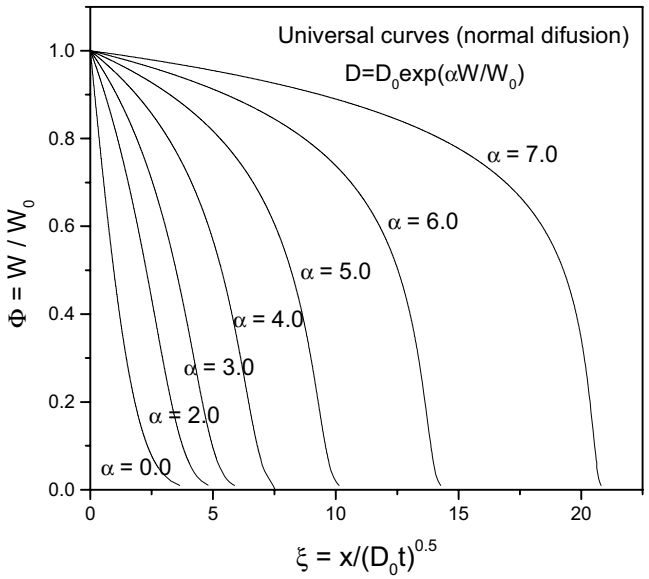

FIG. 1. Numerical solutions $\Phi(\xi)$ of a 1D normal diffusion equation with a concentration-dependent transport diffusivity of form $D(W)=D_0\exp(\alpha\Phi)$ for various values of the parameter α.

Early measurements of water intake in soils [26] revealed that the moisture profiles could be explained by Eq. (1) provided an approximately exponential increase of $D(W)$ with moisture content was assumed. Although, in general, there is little theoretical basis for such an assumption an exponential growth parameter was later employed to approximately characterize the wetting process in other porous systems. However, marked deviations from exponential behavior are apparent in several cases [27].

Assuming $W(0,t)=W_0$ for $t>0$ and $W(x,0)=0$ for $x>0$, and a semiinfinite plane for $x>0$, the boundary conditions, as well as Eq. (1) itself, can be expressed in terms of a single scaling variable through Boltzmann's transformation. Hence, when plotted as a function of this scaling variable all profiles $W(x,t)$ would collapse into a single universal curve.

In order to facilitate the discussion of our results in zeolites we first recalculate the universal curves resulting from Eq. (1) assuming an exponential dependence of form $D(W)=D_0\exp(\alpha W/W_0)$.

Defining a scaling variable $\xi=x/(D_0/t)^{1/2}$, Eq. (1) becomes:

$$-\frac{1}{2}\xi\frac{d\Phi}{d\xi} = \frac{d}{d\xi}\left(\exp(\alpha\Phi)\frac{d\Phi}{d\xi}\right). \tag{2}$$

where $\Phi=W/W_0$ and $\Phi(\xi=0)=1$, $\Phi(\xi\to\infty)=0$.

Figure 1 shows numerical solutions of Eq. (2) represent-

TABLE I. Parameters characterizing the solution $\Phi(\xi)=W/W_0$ of a normal 1D diffusion equation with a concentration-dependent transport diffusivity of form $D(W)=D_0\exp(\alpha\Phi)$. The abscissa ξ_Φ satisfies $\Phi(\xi_\Phi)=1/2$ and $S=(2\xi_\Phi|(d\Phi/d\xi)_{\xi=0}|)^{-1}$.

α	$\lvert(d\Phi/d\xi)_{\xi=0}\rvert\times\sqrt{\pi}$	ξ_Φ	S
0	1	0.97	0.91
1	0.51253	1.48	1.17
2	0.268685	2.27	1.45
3	0.143895	3.49	1.76
4	0.078445	5.43	2.08
5	0.043413	8.17	2.50
6	0.02432	12.52	2.91
7	0.013762	19.25	3.34

ing universal curves $\Phi(\xi)$ for various values of α. The results, obtained by Runge-Kutta's method, are similar to those reported earlier [21]. Moreover, Table I shows additional results including the initial derivative $(d\Phi/d\xi)_{\xi=0}$ for various values of α. Also shown are values of a parameter $S(\alpha)$ which describes to what extent the profiles approximate an advancing rectangular wetting front. A possible choice of such a parameter, which is independent of D_0, is the ratio ξ_s/ξ_Φ. Here ξ_s denotes the abscissa where the initial straight line, with slope $(d\Phi/d\xi)_{\xi=0}$, intersects the horizontal line $\Phi=1/2$, whereas ξ_Φ is the abscissa where $\Phi=1/2$. $S(\alpha)$ defined in this manner, which can be alternatively expressed by $(2\xi_\Phi|(d\Phi/d\xi)_{\xi-0}|)^{-1}$, is expected to become very large as a "rectangular" shape is approached and to have a value $S(\alpha)=1$ for a "triangular" shape. The data of Fig. 1 illustrate the changes in the universal curves as α increases and the correspondence with the values of $S(\alpha)$ listed in Table I.

From a microscopic point of view the chemical potential of the diffusers should approximate the independent particle limit at very low concentration and very low porosity. Provided this limit is experimentally attainable, the transport diffusivity could approach the value of the self-diffusion coefficient determined by drag forces in the random molecular motion of such particles. Although for $W\approx W_0$ the measured transport diffusivity can be orders of magnitude larger than typical self-diffusion coefficients of water, as $W\approx 0$, when vapor transport begins to plays a dominant role in determining liquid transport, values in the range of 10^{-5} cm^2/s or below have been approached [2,27]. However, only an order of magnitude agreement between self-diffusion coefficients and transport diffusivities can, in general, be expected even in this limit.

III. ANOMALOUS DIFFUSION: MOISTURE DEPENDENCE OF THE EFFECTIVE TRANSPORT DIFFUSIVITY

All our NMR imaging measurements of water intake in nonactivated Y-type (Na) zeolite compressed fine powder samples indicated subdiffusive behavior. Scaling variables $\eta=x/t^{\gamma/2}$, with $\gamma<1$ were needed, in all cases, for collapsing the profiles into universal curves. From the point of view of fractal time Brownian motion subdiffusive behavior originates in a random walk with random waiting times T_i between successive jumps and a probability distribution [28] of waiting times characterized by a long tail $P(T_i>t)=At^{-\gamma}(0<\gamma<1)$ with a mean value $\langle T_i\rangle=\infty$. Moreover, for diffusion in a percolating cluster, the value of γ is expected to be determined by the fractal dimension of the cluster [29,30].

We have recently employed [3] a Riemann-Liouville fractional derivative approach to the FTD equation to derive an expression for calculating the moisture dependence of the effective transport diffusivity $D_\gamma(W)$(cm^2/s$^\gamma$). For normal $(\gamma=1)$ diffusion such an expression follows immediately from Boltzmann's transformation of the diffusion equation [1]. For $\gamma<1$ the equivalent expression can be shown to have the form [3]

$$D_\gamma(\eta)=\frac{d\eta}{d\Phi}\frac{1}{\Gamma(1-\gamma)}\int_\infty^\eta d\eta'\int_{\eta'}^\infty\left[(2/\gamma)(1-\gamma)\frac{\Phi(\lambda)}{\lambda}-\frac{d\Phi(\lambda)}{d\lambda}\right]\frac{(\eta'/\lambda)^{2/\gamma}d\lambda}{(1-(\eta'/\lambda)^{2/\gamma})^\gamma},\tag{3}$$

where $\Phi(\eta)=W(\eta)/W_0$ represents the universal curve obtained from the experimentally determined moisture profiles when plotted as a function of the scaling variable $\eta=x/t^{\gamma/2}$.

Equation (3) implicitly yields, for anomalous diffusion, the moisture dependence of the effective transport diffusivity $D_\gamma(W)$ from water intake profiles determined by NMR imaging. As a check of the consistency of Eq. (3) two special cases can be considered. For $\Phi(\xi)=1-\mathrm{erf}(\xi/2)$ with $\xi=x/(D_0t)^{1/2}$, corresponding to the solution of Eq. (2) for a constant diffusivity D_0 (i.e., $\alpha=0$), Eq. (3) approaches, as expected, a constant value of D_γ as $\gamma\to 1$. Moreover, if one adopts for $\Phi(\xi)$ the known solution of the FTD equation with a constant effective diffusivity, assuming Boltzmann's boundary conditions, a constant value of D_γ is also obtained [3] for any value of γ.

IV. RESULTS AND DISCUSSION

The nonactivated samples used in our experiments [3] were cylindrical rods with 5 cm in diameter and length varying between 5.0 and 6.0 cm. The sample preparation procedure deserves special attention since activated zeolites readily adsorb water molecules into their intracrystalline pores liberating a considerable amount of heat that could affect the water transport process. The starting material was Y (Na) zeolite (Aldrich, lot 13 322 PU, average diameter: 6 μm with a dispersion of ± 2 μm). This dry fine powder was first moisturized using a vaporizer causing a considerable release of heat of adsorption. When no further heating was observable, the somewhat moist material was placed in a steel mold under an applied pressure of up to 15 MPa and dried to remove any excess of nonadsorbed liquid water. This could be confirmed by the absence of a liquid water NMR signal.

The water removal procedure in materials like zeolites containing intracrystallite pores of nanometric diameter, is especially sensitive to a form of damage called steaming.

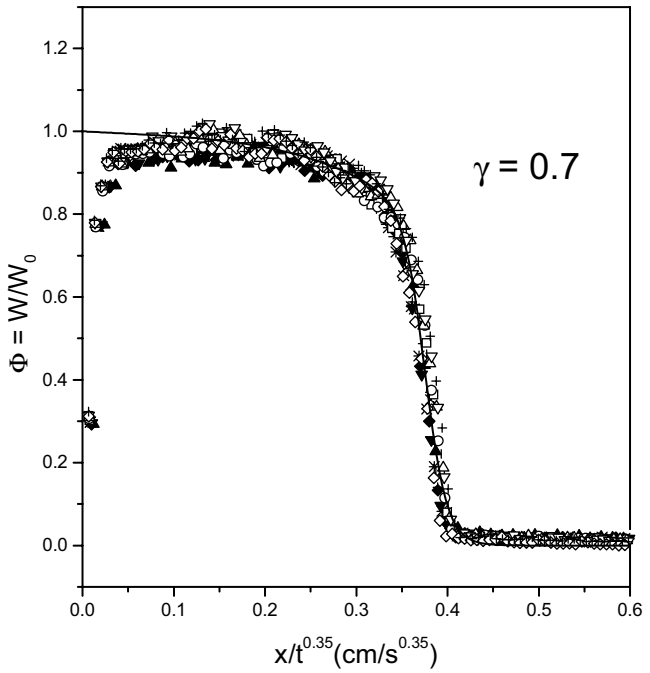

FIG. 2. Universal curve involving various profiles obtained at times from 2 min$\leqslant t \leqslant$40 min in a recycled nonactivated zeolite sample. The data are plotted as a function of $\eta = x/t^{0.35}$ and the solid line represents an empirical fitting function.

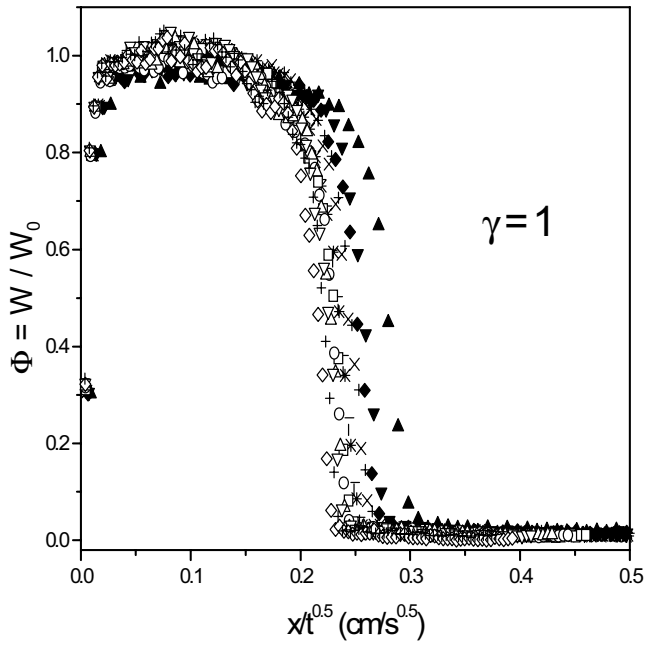

FIG. 3. Same data as in Fig. 2 plotted as a function of $x/t^{0.5}$ showing the departure from normal diffusion.

Steaming occurs when internal vapor pressure causes damage to the structure of the sample. Specifically in the case of zeolites a vaporizing and recondensing of water within the sample causes recrystallization. To avoid steaming [31], moisture from freshly prepared samples was slowly removed at less than 100 °C and then temperature was increased in a stepwise manner up to no more than 140 °C. This was sufficient to remove most liquid water but not enough to remove adsorbed water and activate the zeolite.

Once the sample was dry a water reservoir was placed in contact with one end of the sample and liquid water ingress was monitored, by means of ^{1}H NMR imaging of a narrow concentric cylindrical region of interest [3], until saturation of all intercrystallite pores. We denote as fresh samples those which, after the preparation and drying procedure mentioned above, were placed in contact with a water reservoir for the first time. Samples that had already been exposed to water saturation of the intercrystallite pore space through contact with a reservoir and were later dried and reused, are termed recycled samples.

One of the most notable aspects of these systems is the departure from normal diffusion characterized by values $\gamma < 1$. Another aspect is the strong dependence of the value of γ and also of the shape of the universal curves, characterized by the parameter S defined earlier, on the history of the sample.

Figure 2 shows a typical example of a recycled zeolite sample that, after complete water saturation, was subsequently dried at a temperature of 140 °C for 24 h and subjected to a new water intake, during which no appreciable heating effects were detected. The behavior will be seen to be very different from that of fresh samples, where only a small amount of moisture has been slowly removed, but have never before been exposed to water intake from a reservoir. From Fig. 2 it appears that the data, which includes moisture profiles for times ranging between $t=7$ min and $t=40$ min, approximately collapse into a universal curve when the moisture profiles are plotted as a function of the scaling variable $x/t^{0.35}$, corresponding to $\gamma=0.7$. Also shown in Fig. 2 is an empirical fitting function that can be adjusted to fit the range of data not affected by an initial experimental artifact [3]. For all our zeolite systems we found that a good adjustment could be obtained by a product of a $\gamma=1$ constant diffusivity solution times an apodizing function. The general form of this fitting function is:

$$\Phi_{\mathrm{adj}}(\eta) = [1 - \mathrm{erf}(\eta/\varepsilon)]\exp[-(\delta\eta)^{\mathrm{m}}][1/(1+(\beta\eta)^{\mathrm{n}})],$$

where ε, δ, and β are adjustable parameters and n, m are adjustable integers. For the fitting of Fig. 2 the following values have been used $\varepsilon=10$, $\delta=1.785$, $\beta=2.653$ with $n=32$, and $m=4$.

Figure 3 shows the same data of Fig. 2 now plotted as a function of $x/t^{1/2}$, corresponding to normal diffusion with $\gamma=1$. It is clear that the data do not collapse into a universal curve when plotted in this manner, indicating anomalous diffusion.

Values of γ in the range of 0.64 to 0.8 were found among the many recycled Y-type (Na) zeolite samples examined.

Although the data of Fig. 2 indicate a value of γ typical of the range above, this universal curve exhibits a particularly pronounced "squareness" ($S \approx 10$). It is worth stressing that values of the parameter S, defined earlier, can differ substantially from this value for other values of γ, and even be different for the same value of γ.

From the total mass of water intake, one concludes that the value of γ in our samples appears to be larger for larger

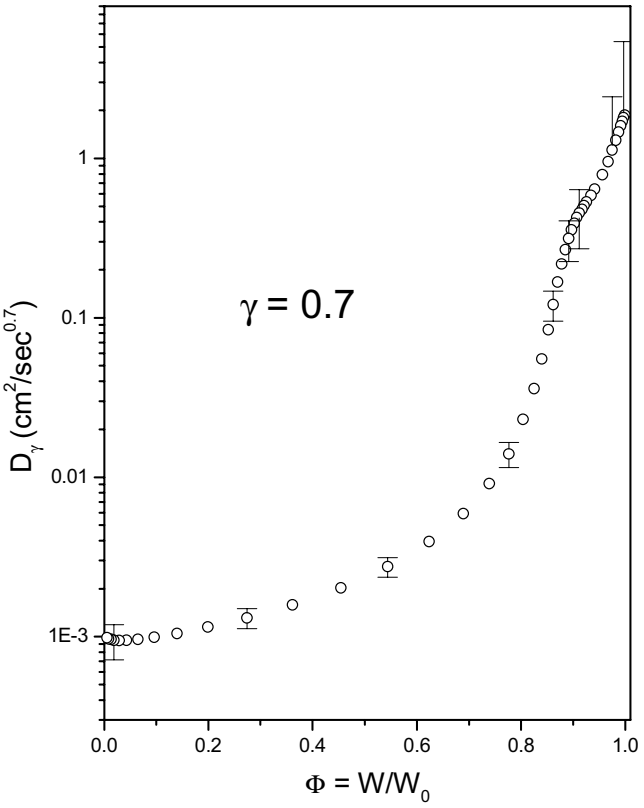

FIG. 4. (◦) Calculated values of $D_\gamma(\Phi)$ obtained from Eq. (3) using the data of Fig. 2.

porosity samples but appears not to be correlated with the value of S. On the other hand, as expected also for normal diffusion, the value of the parameter S appears to increase with the tortuosity of the pore space. The broadening of the pore diameter distribution may be the result of damage caused by water intake and subsequent removal.

The moisture dependence of the effective transport diffusivity can be obtained by the integral of Eq. (3) with $\Phi(\eta)$ given by the fitting function $\Phi_{\text{adj}}(\eta)$ of Fig. 2. The result is shown in Fig. 4 where typical error bars have been determined by varying the fitting function within the uncertainties of the data. These uncertainties are larger for $\Phi_{\max} \approx 1$, because of the experimental artifact affecting the beginning of the profiles [3], and for $\Phi_{\min} \approx 0$ as a result of the poor signal to noise ratio in this region. Figure 4 shows that the effective transport diffusivity grows monotonically with moisture content but departs considerably from a single exponential. The fast growth for $\Phi \geqslant 0.8$ may explain the large value of S compared with the data of Table I. Nonexponential growth, somewhat resembling Fig. 4, has been observed before for $\gamma=1$ in systems like gypsum [27].

Even for a nonexponential but monotonic growth it is convenient to define, a parameter $\alpha=\ln[D_\gamma(\Phi_{\max})/D_\gamma(\Phi_{\min})]$ representing the total variation of the effective diffusivity. From the data of Fig. 4 the value of α can be found to be in the range 7.5 to 8.4.

Fresh Y-type (Na) zeolite samples should in principle have a narrower distribution of pore diameters than samples subjected to damage caused by forced water removal after

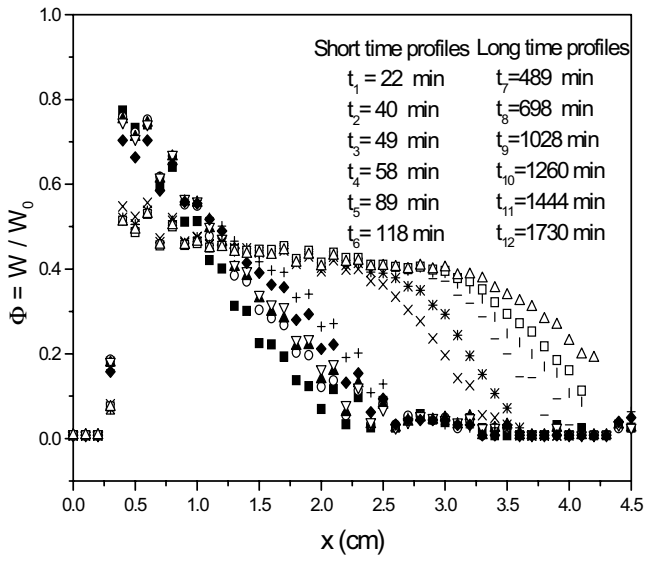

FIG. 5. Water content profiles along the cylindrical x axis obtained at various times in a fresh nonactivated zeolite sample which has been subjected to a pressure of 15 MPa. Two different regimes are clearly distinguishable: A short time regime (22 min $< t <$ 118 min), and a long time regime (489 min $< t <$ 1730 min).

saturation. As a consequence, smaller values of α can generally be expected, as confirmed by our experiments. Subdiffusive behavior was also observed in all fresh samples with lower values of porosity samples exhibiting lower values of γ. Of particular interest is, a Y-type (Na) zeolite sample, prepared under an applied pressure of 15 MPa, which exhibited a value $\gamma=0.4$. Water ingress in this sample was so slow that profiles could be monitored for approximately 29 h as shown in Fig. 5.

The profiles shown in Fig. 5 can be divided into two groups characterized by quite different values of the parameter S. For clarity, the transition region between short time profiles and long time profiles has been suppressed. Moreover, since end effects may invalidate the conditions of Boltzmann's transformation, data for $x \geqslant 4.3$ cm were also suppressed for the longest time profile in Fig. 5.

The data of Fig. 5 indicate that a diffusion equation with a single diffusivity, dependent only on water concentration W, is not applicable over the whole time domain. Moreover, the loss in signal amplitude for longer times suggests that an intermediary relaxation process might be involved. It appears to be possible to separate the process into two regimes: A short time regime, where the relaxation has not yet affected appreciably the diffusion process, and a long time regime where the relaxation process has been completed and further evolution is governed by diffusion only. The short time regime in this sample, with a quoted value $\gamma=0.36\pm0.4$, has been analyzed in detail earlier [3].

A quite remarkable result is that, within the experimental uncertainty, the short time regime and the long time regime scale with the same value of γ. Invoking a possible analogy with diffusion in a percolating cluster, the above result would suggest that the fractal dimension of the random walk [29] in the cluster is not affected by other ongoing processes which appear to modify some other aspects of the pore structure.

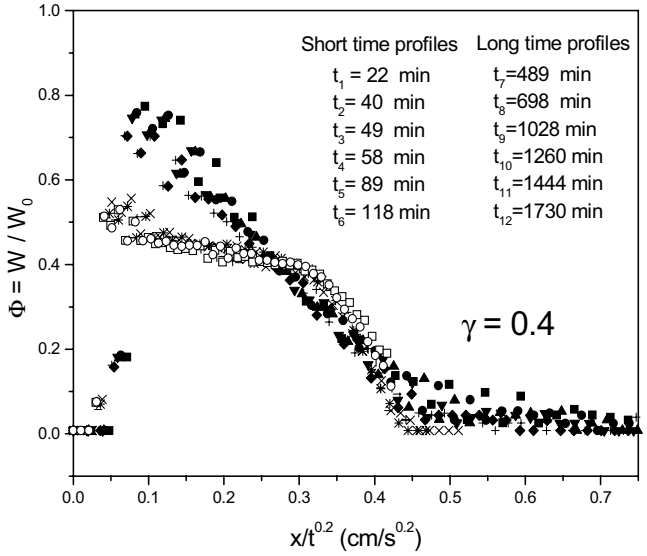

FIG. 6. Universal curves resulting from the profiles of Fig. 5 when plotted as a function of $x/t^{0.2}$. The short time regime (22 min$<t<$118 min) and the long time regime (489 min$<t<$1730 min) are clearly distinguishable.

Figure 6, where the data of Fig. 5 are plotted as a function of the scaling variable $\eta=x/t^{0.2}$, shows a collapse into two different universal curves for the same value of $\gamma=0.4$. When the same data are plotted as a function of $x/t^{1/2}$, as in Fig. 7, no such collapse is observable indicating anomalous diffusion.

It is apparent from Fig. 6 that the short time regime relaxes toward a long time regime where, from the shape of the profiles, the moisture dependence of the effective diffusivity displays a more rapid growth. Furthermore the loss in signal amplitude during relaxation suggests an unbalance between the rate of liquid water vaporization and vapor condensation. One could argue that part of the liquid water vaporizing per unit time is adsorbed into nanopores of the zeolite and is not

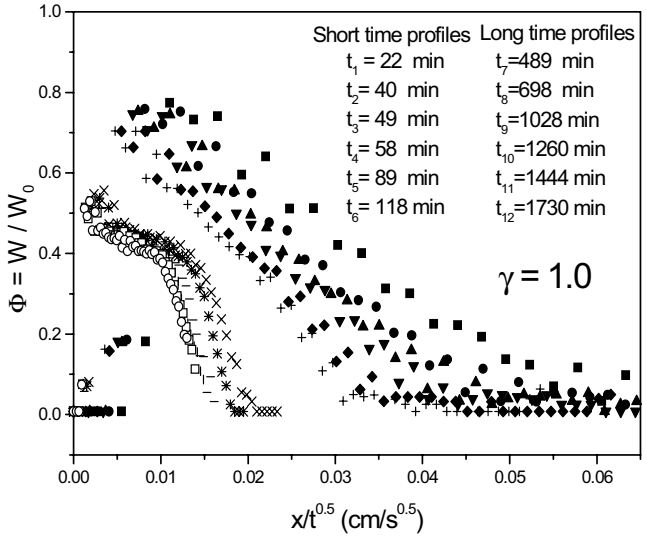

FIG. 7. Same data as in Fig. 6 plotted as a function of $x/t^{0.5}$ showing the departure from normal diffusion.

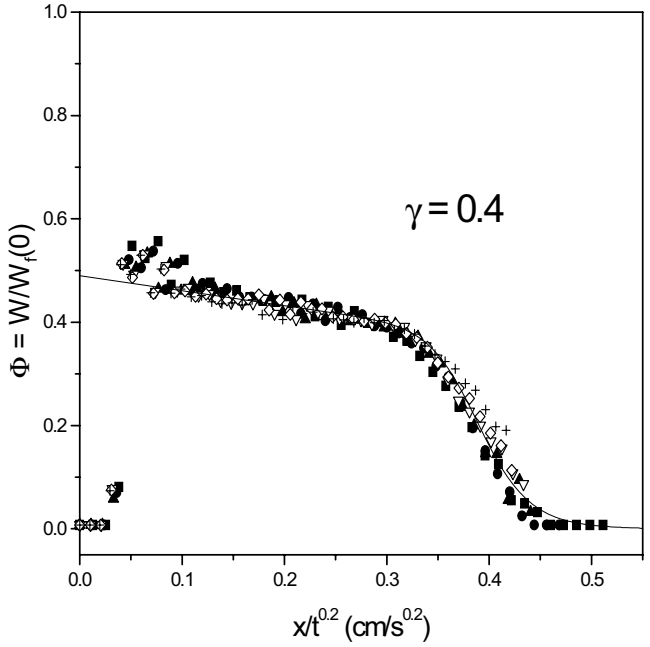

FIG. 8. Universal curve corresponding to the long time regime of Fig. 6 with the data plotted as a function of $\eta=x/t^{0.2}$. The solid line represents an empirical fitting function.

reconverted into liquid. This could be caused by the presence of residual adsorption sites which were not filled during the sample preparation procedure. Another possibility is that a lattice relaxation [32], caused by the rather prolonged contact of the adsorbate with the adsorbent in this particular sample, might have occurred. This may have created new adsorption sites and could explain the observed change in the transport mechanism after the relaxation. It is worth pointing out that, as in all samples studied, no appreciable heating was observed during the relaxation process or thereafter. Furthermore, since adsorbed molecules are expected to be more tightly bound than liquid water molecules the process tends to shorten the spin-spin relaxation time T_2 and cause the observed signal loss. From the rate of signal loss we can estimate a characteristic time of the relaxation process of approximately 300 min.

The data of Fig. 5 suggest that the relaxation process leads to a configuration of mesopores with a more pronounced tortuosity of the pore space which actually changes the nature of the transport. This is suggested by the larger value of the parameter S_{Lt} in the long time regime. Moreover, we can use Eq. (3) to correlate the moisture dependence of the effective transport diffusivity with the parameter S characterizing the shape of the profiles. Figure 8 shows the universal curve obtained by plotting the long time data $\Phi=W/W_{\mathrm{f}}(0)$ of Fig. 6 as a function of $x/t^{0.2}$ together with the empirical fitting function $\Phi_{\mathrm{adj}}(\eta)$ described earlier with parameters $\varepsilon=1.9$, $\delta=0$, $\beta=2.545$, and $n=16$. From the integral of Eq. (3), using the fitting function Φ of Fig. 8, one obtains the moisture dependence of the effective diffusivity shown in Fig. 9.

The shape of the moisture dependence of D_γ in Fig. 9 is similar to that of Fig. 4 but with a smaller value of $\alpha=\ln[D_\gamma(\Phi_{\max})/D_\gamma(\Phi_{\min})]\approx 5.66$. A smaller value of

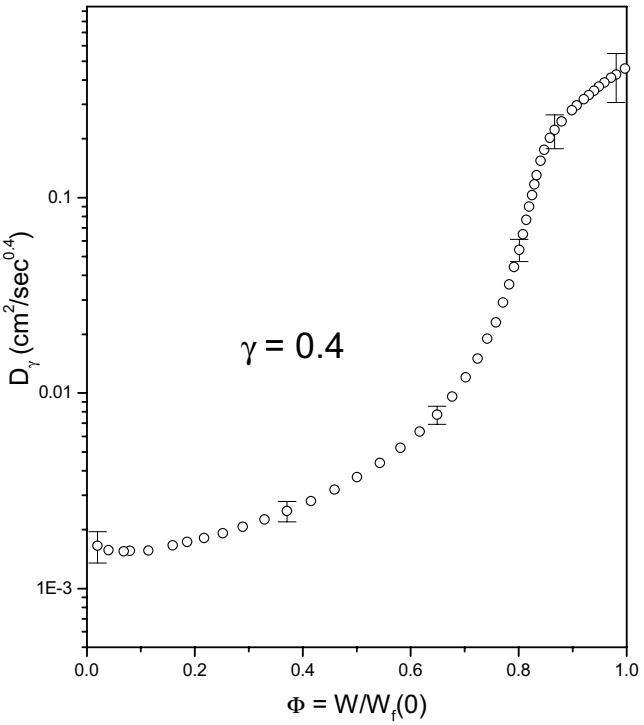

FIG. 9. (◦) Calculated values of $D_\gamma(\Phi)$ obtained from Eq. (3) using the data of Fig. 8.

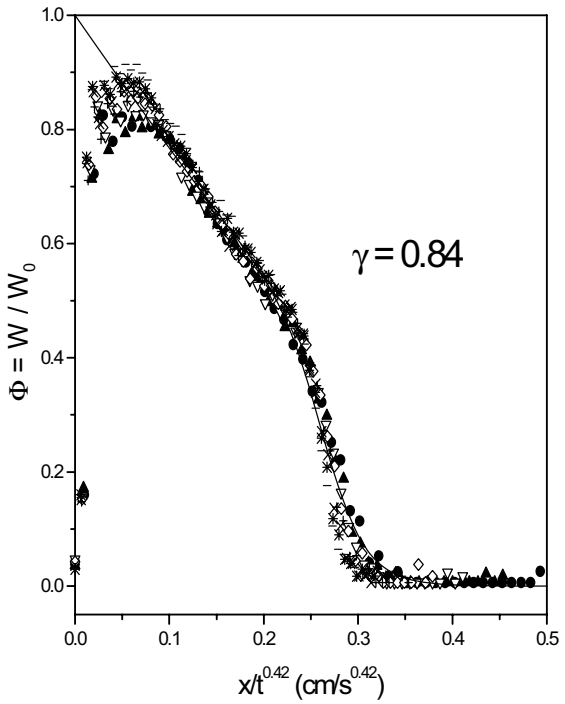

FIG. 10. Universal curve resulting from various profiles obtained at times ranging from 3 min$\leqslant t \leqslant$15 min in a second fresh zeolite sample. The data are plotted as a function of $\eta = x/t^{0.42}$ and the solid line represents an empirical fitting function.

α should actually be expected since, from the shape of the universal curve of Fig. 8, a considerably smaller value $S_{Lt}=2.19$ is obtained. However, it is not possible to directly correlate values of the parameter S with values of α unless they correspond the same value of γ. As an example if the scaling variable in the universal curve of Fig. 8 were assumed to be $x/t^{\gamma/2}$ with $\gamma=0.7$ rather than $\gamma=0.4$ a value $\alpha=4.68$ would have been obtained from Eq. (3) rather than $\alpha=5.66$. Hence the same value of S would correspond to a larger value of α for than for $\gamma=0.7$.

The universal curve corresponding to the short time regime of Fig. 6 and the moisture dependence of the effective transport diffusivity have been examined earlier [3]. For $\gamma=0.4$ we obtained $\alpha=2.10$ with $S_{st}=1.1$, which should be compared with $\alpha=5.66$ and $S_{Lt}=2.19$ for the long time regime curve with the same value of $\gamma=0.4$. The trend can be seen to be similar to that of Table I. but, since the measured moisture dependences do not exhibit a purely exponential growth, the numerical values are not directly comparable.

It is worth mentioning that although recycled samples generally exhibit larger values of α in subsequent water intake experiments, it is possible, in some cases, to obtain a reversible behavior. We were able, for example, to reproduce approximately the same results obtained for the fresh sample of Fig. 6 by a very mild recycling procedure consisting of leaving the saturated sample in a dry environment for several weeks at room temperature and then removing the little excess moisture by slowly increasing the temperature to a maximum of 140 °C.

It is interesting to compare the data of Fig. 6 with those of another freshly prepared, more porous, Y-type (Na) zeolite where the pressure applied to the fine powder during preparation was substantially smaller. Figure 10 shows the universal curve obtained when the profiles are plotted as a function of the scaling variable $x/t^{0.42}$ corresponding to $\gamma=0.84$. The water ingress process in this more porous sample was two orders of magnitude faster than in Fig. 6 and the total water intake, as measured by the mass difference after saturation, was six times larger. Furthermore, since the profiles in Fig. 10 correspond to times between 3–15 min, the relaxation process present in Fig. 6, with a characteristic time of 300 min, could not be observed.

Figure 10 also shows an empirical fitting function, of the general form $\Phi_{adj}(\eta)$ defined earlier, with parameters $\varepsilon=0.478$, $\delta=0$, $\beta=3.673$, and $n=12$. From this fitting function and the integral of Eq. (3), the moisture dependence of the effective transport diffusivity was calculated as shown in Fig. 11. A value $\alpha=\ln[D_\gamma(\Phi_{max})/D_\gamma(\Phi_{min})]=2.68$ with $S=1.0$ was obtained from the data of Fig. 10 and Fig. 11.

The moisture dependences of the effective transport diffusivities D_γ predicted by Eq. (3) for $\gamma<1$ and their connection with the shape of the universal curves appear to be natural extensions of the case $\gamma=1$. Furthermore, the range of values spanned by scaling variables $x/t^{\gamma/2}$ is remarkably similar in all universal curves in spite of pronounced differences in the times involved as well as in the shapes.

V. CONCLUSIONS

The results of Sec. IV are representative of a number of NMR imaging experiments performed in a large variety

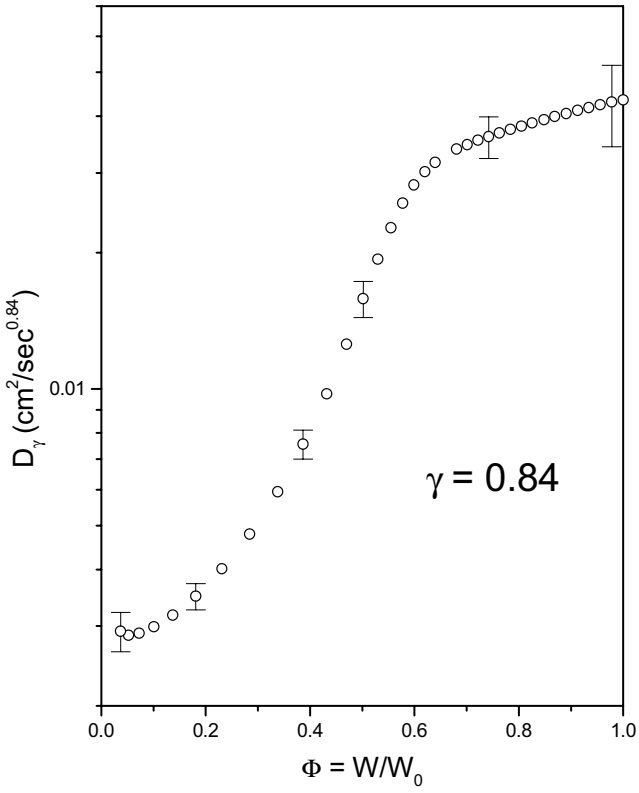

FIG. 11. (◦) Calculated values of $D_\gamma(\Phi)$ obtained from Eq. (3) using the data of Fig. 10.

of Y-type (Na) zeolite samples prepared under different conditions. The ubiquitous presence of subdiffusive behavior led us to adopt a FTD equation, which proved to be a very useful framework to describe the data. Using Eq. (3), derived from the FTD equation with boundary conditions appropriate for Boltzmann's transformation, valuable results could be obtained for any value of γ ($\gamma<1$). As in normal ($\gamma=1$) diffusion, the parameter $\alpha=\ln[D_\gamma(\Phi_{\max})/D_\gamma(\Phi_{\min})]$, characterizing the growth of the effective transport diffusivity with moisture content, has been found to determine the shape of the universal curves, as described by the parameter S. As α increases so does S but the relationship is different for different values of γ. The smaller γ the larger α for a given S. Moreover, the data indicate that γ and α might not be correlated, as shown most vividly by Fig. 6.

The FTD equation also permits, for $\gamma<1$, to correlate water intake profiles with structural changes taking place in the mesopore / nanopore structure. Fresh samples exhibit values of $\alpha=2.1-2.7$, independent of the value of γ. However, after prolonged contact between adsorbate and adsorbant, a lattice relaxation process could be taking place leading to a larger value $\alpha=5.66$. Forced removal of water after saturation appears to generally increase the porosity and further broaden the distribution of pore diameters, but does not restore the initial conditions unless very special care is taken.

From a qualitative point of view, a distinctive aspect of water transport in our zeolite samples, as opposed for example to fired-clay brick, mortar, and other similar porous systems displaying normal diffusive behavior, may be related to very slowly decaying structural changes caused by water intake. This has been recognized as a precondition for anomalous diffusion [1]. Irreversible changes in the mesopore / nanopore structures that occur as water ingresses into a fine particle zeolite powder compacted by high pressure could arguably be responsible for anomalous behavior. On the other hand subdiffusive behavior has been recently observed [29] in quite different and very well controlled systems consisting of machined random-site percolation model objects. Here subdiffusion has been shown to be specified by the fractal dimension of the random walk, linked to the porosity of the percolating cluster. Although the FTD equation provides a powerful tool for the interpretation of our data, an understanding of the connection between the underlying stochastic model leading to the FTD equation and the origin of subdiffusive behavior in our zeolite samples requires further experimental and theoretical work.

ACKNOWLEDGMENTS

We wish to thank Mirla de N. do N. Miranda and Maria Aparecida Silva for helpful comments. This work has been supported by Conselho Nacional de Desenvolvimento Científico e Tecnológico and by PETROBRAS.

[1] J. Crank, *The Mathematics of Diffusion* (Oxford University Press, London, 1975).
[2] S. Blackband and P. Mansfield, J. Phys. C **19**, L49 (1986).
[3] E. N. de Azevedo, P. L. de Souza, R. E. de Souza, M. Engelsberg, M. de N. do N. Miranda, and M. Aparecida Silva, Phys. Rev. E **73**, 011204 (2006).
[4] R. Metzler, E. Barkei, and J. Klafter, Phys. Rev. Lett. **82**, 3563 (1999).
[5] R. Metzler and J. Klafter, Phys. Rep. **339**, 1 (2000).
[6] E. Barkai, R. Metzler, and J. Klafter, Phys. Rev. E **61**, 132 (2000).
[7] R. Metzler and T. F. Nonnenmacher, Chem. Phys. **284**, 67 (2002).
[8] R. Hilfer, J. Phys. Chem. B **104**, 3914 (2000).
[9] W. L. Vargas, L. E. Palacio, and D. M. Dominguez, Phys. Rev. E **67**, 026314 (2003).
[10] E. K. Lenzi, R. S. Mendes, and C. Tsallis, Phys. Rev. E **67**, 031104 (2003).
[11] C. H. Rüsher, N. Salman, J.-Chr. Buhl, and W. Lutz, Microporous Mesoporous Mater. **92**, 309 (2006).
[12] D. W. Breck, *Zeolite Molecular Sieves* (John Wiley & Sons, London, 1974).
[13] J. Kärger and D. M. Ruthven, *Diffusion in Zeolites and Other Microporous Solids* (John Wiley, New York, 1992).
[14] E. O. Stejkal and J. E. Tanner, J. Chem. Phys. **42**, 288 (1965).
[15] P. T. Callaghan, *Principles of NMR Microscopy* (Clarendon

Press, Oxford, 1991).
[16] R. Kimmich, *NMR Tomography, Diffusometry, Relaxometry* (Springer-Verlag, Berlin, 1997).
[17] R. Krishna and J. Wesselingh, Chem. Eng. Sci. **52**, 861 (1997).
[18] Vishwas Gupta, Sriram S. Nivarthi, Alon V. McCormick, and H. Ted Davis, Chem. Phys. Lett. **247**, 596 (1995).
[19] K. Hahn, J. Kärger, and V. Kukla, Phys. Rev. Lett. **76**, 2762 (1995).
[20] Tom Chou, Phys. Rev. Lett. **80**, 85 (1997).
[21] H. P. G. Darcy, *Les Fontaines Publiques de La Ville du Dijon* (Delmont, Paris, France 1856).
[22] J. Bear and Y. Bachmat, *Introduction to Modeling of Transport Phenomena in Porous Media* (Kluwer Dordrecht, The Nederlands 1990), Vol. 4.
[23] Y. Mualem, Water Resour. Res. **10**, 514 (1974).
[24] L. Pel, H. Brocken, and K. Kopinga, Int. J. Heat Mass Transfer **39**, 1273 (1996).
[25] L. Pel, K. Kopinga, G. Betram, and G. Lang, J. Phys. D **28**, 675 (1995).
[26] W. R. Gardner and M. S. Mayhugh, Soil Sci. Soc. Am. Proc. **22**, 197 (1958).
[27] L. Pel, Ph.D. thesis (Eindhoven University of Technology, The Nederlands, 1995).
[28] Karina Weron and Marcin Kotulski, Physica A **232**, 180 (1996).
[29] Andreas Klemm, Ralf Metzler, and Rainer Kimmich, Phys. Rev. E **65**, 021112 (2002).
[30] S. Alexander and R. Orbach, J. Phys. (France) Lett. **43**, L-625 (1982).
[31] P. A. Webb and C. Orr, *Analytical Methods in Fine Particle Technology* (Micromeritics Instrument Corporation, Norcross, 1997), p. 130.
[32] J. J. I. Van Dun, W. J. Mortier, and J. B. Uytterhoeven, Zeolites **5**, 257 (1988).